Crystal Structure of *Escherichia coli* Crotonobetainyl-CoA: Carnitine CoA-Transferase (CaiB) and Its Complexes with CoA and Carnitinyl-CoA†

Erumbi S. Rangarajan,‡,§ Yunge Li,§,|| Pietro Iannuzzi,§,|| Miroslaw Cygler,‡,§,|| and Allan Matte*,§,||

Department of Biochemistry, McGill University, Montreal, Quebec, Canada, Montreal Joint Center for Structural Biology, Montreal, Quebec, Canada, and Biotechnology Research Institute, National Research Council of Canada, 6100 Royalmount Avenue, Montreal, Quebec H4P 2R2

Received November 3, 2004; Revised Manuscript Received January 19, 2005

ABSTRACT: L-Carnitine (*R*-[−]-3-hydroxy-4-trimethylaminobutyrate) is found in both eukaryotic and prokaryotic cells and participates in diverse processes including long-chain fatty-acid transport and osmoprotection. The enzyme crotonobetainyl/γ-butyrobetainyl-CoA:carnitine CoA-transferase (CaiB; E.C. 2.8.3.-) catalyzes the first step in carnitine metabolism, leading to the final product γ-butyrobetaine. The crystal structures of *Escherichia coli* apo-CaiB, as well as its Asp169Ala mutant bound to CoA and to carnitinyl-CoA, have been determined and refined to 1.6, 2.4, and 2.4 Å resolution, respectively. CaiB is composed of two identical circular chains that together form an intertwined dimer. Each monomer consists of a large domain, containing a Rossmann fold, and a small domain. The monomer and dimer resemble those of formyl-CoA transferase from *Oxalobacter formigenes*, as well as *E. coli* YfdW, a putative type-III CoA transferase of unknown function. The CoA cofactor-binding site is formed at the interface of the large domain of one monomer and the small domain from the second monomer. Most of the protein−CoA interactions are formed with the Rossmann fold domain. While the location of cofactor binding is similar in the three proteins, the specific CoA−protein interactions vary somewhat between CaiB, formyl-CoA transferase, and YfdW. CoA binding results in a change in the relative positions of the large and small domains compared with apo-CaiB. The observed carnitinyl-CoA product in crystals of the CaiB Asp169Ala mutant cocrystallized with crotonoyl-CoA and carnitine could result from (i) a catalytic mechanism involving a ternary enzyme−substrate complex, independent of a covalent anhydride intermediate with Asp169, (ii) a spontaneous reaction of the substrates in solution, followed by binding to the enzyme, or (iii) an involvement of another residue substituting functionally for Asp169, such as Glu23.

L-Carnitine (*R*-[−]-3-hydroxy-4-trimethylaminobutyrate) plays various important functions within eukaryotic and prokaryotic cells. In eukaryotes, carnitine is used in the transport of long-chain fatty acids across the inner mitochondrial membrane (*1*). In prokaryotes, carnitine, along with other betaines, serves as an osmoprotectant (*2*) and in some cases as a growth stimulant (*3*). There is also interest in the industrial, enzymatic-based synthesis of L-carnitine (*4*) because this compound has a variety of medical applications (*5*).

Carnitine metabolism in bacteria can proceed by one of three possible routes (*6*). Some organisms, such as *Pseudomonas* species, utilize carnitine as a sole source of carbon and nitrogen (*6*), while a second group degrades only the carbon backbone to yield the product trimethylamine (*7*). The third route, utilized by *Escherichia coli*, does not result in assimilation of carnitine; instead, it is converted to γ-butyrobetaine via the formation of crotonobetaine (Figure 1). The genes comprising the proteins of the *E. coli* carnitine pathway, *caiTABCDE*, form a single operon that is transcribed under anaerobic conditions and is induced by carnitine (*8*). CaiT is a putative carnitine transporter, while Cai_{A-E} are metabolic enzymes associated with carnitine metabolism. A sixth protein, CaiF, is not part of this operon but functions as a carnitine-sensitive transcriptional regulator of the *cai* and *fix* operons (*9*).

CaiB catalyzes the first step in carnitine metabolism, leading finally to the product γ-butyrobetaine. This enzyme had originally been designated as carnitine dehydratase (E.C. 4.2.1.89; *10*, *11*) but does not possess this activity and has been subsequently recharacterized as a CoA transferase that utilizes crotonobetainyl-CoA, γ-butyrobetainyl-CoA, or carnitinyl-CoA and their respective betaines, crotonobetaine, γ-butyrobetaine, or L-carnitine (E.C. 2.8.3.-; *12*; Figure 1). The dehydration of L-carnitinyl-CoA to crotonobetainyl-CoA is not catalyzed by CaiB but by a second enzyme, carnitinyl-CoA dehydratase (CaiD; E.C. 4.2.1.-; *12*). Both crotonobetainyl-CoA and γ-butyrobetainyl-CoA are new CoA derivatives that have only been recently identified and characterized (*13*). CaiB is a homodimeric enzyme and has been purified and characterized from *E. coli* (*13*) and *Proteus vulgaris* (*14*).

† This research was funded by a grant from the Canadian Institutes of Health Research, 200103GSP-90094-GMX-CFAA-19924 to M.C.

* To whom correspondence should be addressed: Biotechnology Research Institute, 6100 Royalmount Avenue, Montreal, Quebec H4P 2R2, Canada. Telephone: 514-496-2557. Fax: 514-496-5143. E-mail: allan.matte@nrc-cnrc.gc.ca.

‡ McGill University.

§ Montreal Joint Center for Structural Biology.

|| National Research Council of Canada.

10.1021/bi047656f CCC: $30.25
Published on Web 03/23/2005

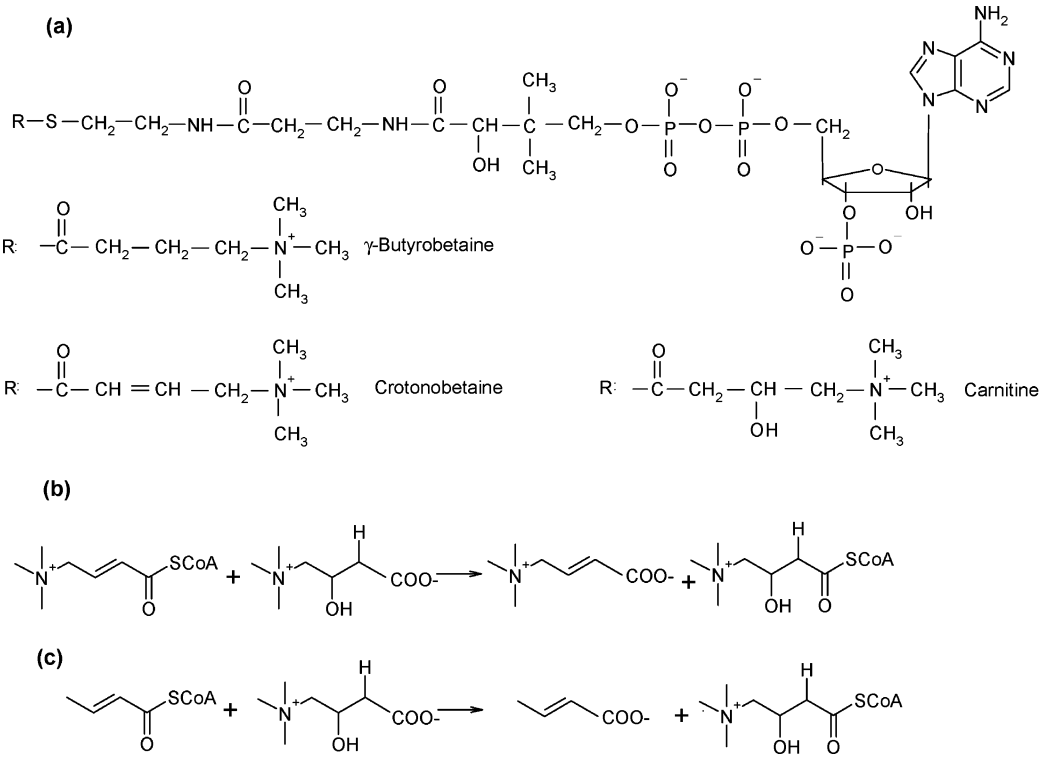

FIGURE 1: CoA-transferase reaction catalyzed by *E. coli* CaiB and its associated CoA cosubstrates. (a) Chemical structures of CoA and CoA derivatives referred to in this paper. The groups (R:) attached to CoA yields the ligands γ-butyrobetainyl-CoA, crotonobetainyl-CoA, and carnitinyl-CoA. (b) Schematic diagram showing the chemical reaction catalyzed by CaiB (*12*). Here, the CoA moiety of crotonobetainyl-CoA is transferred to carnitine, yielding free crotonobetaine and carnitinyl-CoA. (c) Proposed reaction leading to formation of carnitinyl-CoA observed in crystals of CaiB cocrystallized with crotonoyl-CoA and carnitine. Figures were prepared using ISIS DRAW (www.mdl.com).

CoA-transferases have been grouped into three distinct families based on amino acid sequence, biochemical, and mechanistic criteria (*15*). Family I consists of hetero-oligomeric enzymes that use acetyl-CoA or succinyl-CoA as CoA donors and that operate with a ping-pong kinetic mechanism. Family II contains only a few members, including citrate lyase (E.C. 2.8.3.10) and citramalate lyase (E.C. 2.8.3.11). Family III has been identified more recently (*15*) and contains formyl-CoA:oxalate CoA transferase (E.C. 2.8.3.16; *16*), succinyl-CoA:(*R*)-benzylsuccinate CoA-transferase (E.C. 2.8.3.15; *17*), (*E*)-cinnamoyl-CoA:(*R*)-phenyllactate CoA-transferase (E.C. 2.8.3.17; *18*), and butyrobetainyl-CoA:(*R*)-carnitine CoA-transferase (CaiB, E.C. 2.8.3.-; *12*). The family III CoA transferases are classified within PFAM PF02515 (PFAM database; *19*) and include the bile-acid-inducible operon protein F (BaiF), a bile acid-CoA hydrolase (*20*).

Crystal structures have been obtained for formyl-CoA transferase from *Oxalobacter formigenes* in apo- and CoA-bound forms (*21*) and a putative formyl-CoA transferase, YfdW, from *E. coli* in an apo form and as a ternary complex bound to CoA (*22*) and to oxalate and acetyl-CoA (*23*). These enzymes form unusual, intertwined dimers, with each monomer forming a ring with a large hole in the center through which the other monomer is threaded. This architecture presents an unusual folding problem that nevertheless has been solved in nature with a range of diverse primary sequences that retain less than 25% identity to one another. Recently, site-specific mutagenesis and crystallographic trapping of the covalent acyl-enzyme intermediate of formyl-CoA transferase from *O. formigenes*, in which Asp169 forms an oxalyl-aspartyl anhydride, have been used to determine its catalytic mechanism (*24*). Here, we report the crystal structure of *E. coli* CaiB in the apo form and in complex with bound CoA. We have also determined the structure of the Asp169Ala mutant cocrystallized with both crotonoyl-CoA and carnitine where, surprisingly, we identified bound carnitinyl-CoA, the product of the reaction. This is the third member of the class III CoA transferase family to be structurally characterized, revealing a similar overall fold and mode of cofactor binding. The complex with carnitinyl-CoA reveals the interactions between CaiB and the betainyl moiety of the CoA thioester.

EXPERIMENTAL PROCEDURES

Cloning, Expression, and Purification. The *caiB* gene (*25*) was PCR-amplified from *E. coli* MC1061 genomic DNA using Taq DNA polymerase (GE Healthcare) and forward and reverse primers (Hückabel Scientific, Montreal, Quebec, Canada) and cloned into the *Bam*H1−*Nde*1 site of a modified pGEX-4T1 vector yielding an in-frame N-terminal GST fusion protein. The CaiB Asp169Ala mutant was prepared using mutagenic primers according to the Quik-Change protocol (Stratagene) and confirmed by DNA sequencing (BioS&T, Inc., Montreal, Quebec, Canada).

For protein production, a 1.0 L culture of *E. coli* DL41 in LeMaster medium for D-selenomethionine (SeMet)[1] labeling (*26*), or for unlabeled protein, a 0.5 L culture of *E. coli* BL21, containing ampicillin (100 μg/mL), was inoculated with a 100 mL overnight culture and grown for 2 h at 37 °C.

[1] Abbreviations: rmsd, root-mean-square deviation; SeMet, D-selenomethionine; TLC, thin-layer chromatography; TLS, translation-libration-screw.

Isopropyl thiogalactopyranoside (IPTG, Sigma) was added at a final concentration of 0.1 mM, and the culture was continued for 6 h. Cells were harvested by centrifugation (4000*g*, 4 °C, 25 min) and stored at −20 °C.

The cell pellet from a 0.5 L culture was resuspended in 40 mL of lysis buffer (50 mM potassium phosphate at pH 7.8, 0.4 M NaCl, 5% glycerol, 10 mM DTT, and 1% Triton X-100), and the cells were lysed by sonication (8 × 15 s, with 15 s between bursts). Cell debris was removed by ultracentrifugation (100000*g*, 20 min, 4 °C), and the supernatant containing GST-CaiB passed through a DEAE column (2.5 mL bed) equilibrated in lysis buffer. The flow-through from this column was applied to a glutathione-Sepharose column (bed volume = 4 mL) equilibrated in lysis buffer. After application of the protein, the column was washed with 10 bed volumes of 50 mM potassium phosphate at pH 7.8, 0.4 M NaCl, 5% (v/v) glycerol, and 10 mM DTT, followed by 10 bed volumes of 50 mM potassium phosphate at pH 7.8, 1 M NaCl, and 10 mM DTT, and finally 10 bed volumes of 50 mM potassium phosphate at pH 7.5 and 10 mM DTT. The GST beads were then resuspended in 2 mL of the final buffer. Cleavage of the GST fusion protein was carried out by adding bovine thrombin at a ratio of 1:1000 (v/v) and incubating at 23 °C for 2 h. The flow-through fraction, containing cleaved GST fusion protein, was collected. Purified protein was characterized by SDS−PAGE, native PAGE, and dynamic light scattering (DLS) using a DynaPro MSPII molecular sizing instrument (Proterion Corp., Piscataway, NJ).

Crystallization. Crystals of apo-CaiB were obtained by sparse-matrix screening using kits I and II from Hampton Research (Aliso Viejo, CA). A 0.5 μL drop of purified protein (7.7 mg/mL) in buffer (50 mM potassium phosphate at pH 7.8 and 5 mM DTT) was mixed with 0.8 μL of reservoir solution in an Impact microbatch crystallization plate (Hampton Research) covered with paraffin oil using a Hydra II crystallization robot (Matrix Technologies, Walnut Creek, CA). Crystals appeared after 2 days at 21 °C. Optimized crystals of CaiB belonging to space group *P*1 were obtained by mixing 1 μL of protein in buffer with 1 μL of reservoir solution (22.5% [w/v] PEG 8000, 0.1 M Tris-HCl at pH 7.0, and 0.2 M sodium acetate). These crystals have unit cell dimensions $a = 70.8$ Å, $b = 83.2$ Å, $c = 89.9$ Å, $\alpha = 100.4°$, $\beta = 110.0°$, and $\gamma = 100.0°$, with $Z = 4$ and diffract to 1.85 Å resolution. A second crystal form of apo-CaiB was obtained from a reservoir solution containing 12.5% [w/v] PEG 8000, 0.1 M Tris-HCl at pH 7.5, and 200 mM $MgCl_2$. These crystals belong to space group *C*2 and have unit cell dimensions $a = 184.3$ Å, $b = 106.2$ Å, $c = 69.7$ Å, and $\beta = 107.5°$, with $Z = 12$ and diffract to 1.6 Å resolution. Crystals of CaiB cocrystallized with either CoA or crotonoyl-CoA (5 mM) were obtained from well solution containing 1.35 M sodium citrate and 0.1 M Tris-HCl at pH 7.0 after 1 week at 21 °C using 1 μL of 7.7 mg/mL CaiB in buffer and 1 μL of reservoir solution. These crystals belong to space group $P4_12_12$ and have unit cell dimensions $a = b = 87.1$ Å and $c = 164.0$ Å, with $Z = 8$ and diffract to 2.3 Å resolution. Similar conditions were used to obtain crystals of the Asp169Ala mutant of CaiB in the presence of 5 mM butyryl-CoA or crotonoyl-CoA in the presence or absence of carnitine. These crystals diffract to 2.4 Å resolution.

For cryoprotection, crystals were transferred briefly to a reservoir solution supplemented with 10% (v/v) glycerol, picked up in a nylon loop, and flash-cooled in the nitrogen cold stream at 100 K. X-ray diffraction data were collected at beamlines X8C and X25, NSLS, Brookhaven National Laboratory, Upton, NY. Data were recorded using a Quantum 4 CCD detector (Area Detector Systems Corp., Poway, CA) (beamline X8C) or Quantum 315 CCD detector (beamline X25) and integrated and scaled using HKL2000 (*27*).

Structure Determination and Refinement. The crystal structure of apo-CaiB was determined, using *P*1 SeMet-labeled crystals, by a three-wavelength MAD experiment about the Se−K edge (peak, inflection, remote; Table 1). During the initial phasing, a total of 58 of 68 expected Se sites were identified and phases calculated to 2.0 Å resolution using SOLVE (*28*), yielding a figure of merit of 0.61. Automated density modification and model building using RESOLVE (*29*), alternating with refinement using REFMAC (*30*), further improved the electron density map and allowed automated model building of 93% of the expected residues within the asymmetric unit. Manual fitting of the model was performed using the program O (*31*), followed by refinement with REFMAC against all data to 1.85 Å resolution, yielding the final model with a R_{work} of 0.176 and R_{free} of 0.212. To obtain the structure of apo-CaiB from *C*2 crystals or the CaiB-CoA or carnitinyl-CoA complexes, molecular replacement using the model from space group *P*1 was performed using MOLREP (*32*) of the CCP4 suite (*33*). The refinement with REFMAC at 1.6 Å resolution converged at R_{work} of 0.187 and R_{free} of 0.213. No NCS restraints were applied.

The structure of CaiB cocrystallized with crotonoyl-CoA (space group $P4_12_12$) was determined by molecular replacement and showed electron density only for bound CoA. Standard refinement with REFMAC resulted in relatively high *R* factors. Therefore, we applied the translation-libration-screw (TLS) option (*34*, *35*), which led to a substantial decrease in R_{work} and R_{free}, and this option was used for all refinement of models in the tetragonal space group. The refinement at 2.3 Å resolution converged to a R_{work} of 0.198 and R_{free} of 0.237. The Asp169Ala mutant cocrystallized with crotonoyl-CoA was isomorphous to the previous crystals and showed electron density only for the CoA portion clearly ending at the terminal sulfur atom of CoA. This structure was refined at 2.4 Å resolution with a R_{work} of 0.198 and R_{free} of 0.244. When both crotonoyl-CoA and carnitine were cocrystallized with the Asp169Ala mutant, the observed electron density extended beyond the CoA moiety and corresponded very well to the expected structure of carnitinyl-CoA instead. The model containing bound carnitinyl-CoA was refined at 2.4 Å resolution with a R_{work} of 0.205 and R_{free} of 0.252.

TLS refinement of apo-CaiB in the *P*1 or *C*2 crystal forms did not reduce the *R* factors and therefore was not employed in the final refinement. A summary of the data collection and processing statistics of the refined models obtained are presented in Table 1.

Enzyme Activity Measurements. Activity assays with CaiB or CaiB Asp169Ala were performed by detection of products by thin-layer chromatography (TLC) and by LC−ESI−MS (1100 Series LC−MSD, Agilent Technologies, Mississauga, Ontario, Canada). Incubation mixtures contained 20 μg of protein in either 50 mM potassium phosphate buffer at pH

Table 1: X-ray Data Collection and Refinement Statistics

						D169A complexes	
crystal	apo				wild type crotonoyl-CoA	crotonoyl-CoA	crotonoyl-CoA and carnitine
Data Collection							
space group	*P*1		*C*2		$P4_12_12$	$P4_12_12$	$P4_12_12$
unit cell							
a (Å)			70.8	184.3	87.8	86.8	86.6
b (Å)			83.2	106.2	87.8	86.8	86.6
c (Å)			89.9	69.7	164.5	164.1	163.9
α (deg)			100.4	90	90	90	90
β (deg)			110	107.5	90	90	90
γ (deg)			100	90	90	90	90
Z			4	12	8	8	8
wavelength	0.9792	0.9802	0.964	1.1	1.1	1.1	1.1
resolution (Å)	50−1.9 (1.97−1.90)	50−1.88 (1.95−1.88)	50−1.85 (1.92−1.85)	50−1.6 (1.66−1.60)	50−2.3 (2.39−2.30)	50−2.4 (2.5−2.4)	50−2.4 (2.5−2.4)
observed reflections	544 906	542 746	523 077	617 583	174 904	177 290	296 577
unique reflections	140 677	143 813	149 486	168 176	29 328	24 947	25 150
redundancy	3.9	3.9	3.5	3.7	5.9	7.1	11.7
completeness (%)	96.2 (79)	95.1 (70)	95 (69.7)	99.9 (100)	98.1 (99.9)	98 (99.8)	99.7 (100)
R_{sym}	0.093 (0.395)	0.108 (0.384)	0.091 (0.409)	0.083 (0.401)	0.054 (0.567)	0.061 (0.412)	0.062 (0.444)
$I/\sigma I$	11.5 (4.2)	12.3 (4.5)	11.7 (3.4)	12.6 (4.6)	26.7 (3.8)	18.3 (5.9)	19.4 (5.87)
Wilson *B* factor (Å)^2			17.9	15.6	53.7	53.9	47.0
Refinement							
resolution (Å)			48.8−1.85	45.6−1.6	41.1−2.3	43.4−2.4	49.09−2.4
R_{work}			0.176 (134 521)	0.187 (159 525)	0.198 (27 309)	0.198 (25 321)	0.205(23 801)
(number of reflections)							
R_{free}			0.212 (14 911)	0.213 (8476)	0.237 (1457)	0.244 (1265)	0.252 (1274)
(number of reflections)							
B factor (Å^2)							
(number of atoms)							
protein			18.49 (12 576)	18.18 (9561)	54.77 (3028)	52.67 (3024)	50.78 (2999)
solvent			28.91 (1560)	29.09 (1174)	54.41 (80)	50.13 (88)	45.50 (82)
ligands					65.55 (48)	59.27 (48)	70.17 (58)
Ramachandran							
allowed			99.4	99.4	99.3	99.4	98.8
generous			0.4	0.5	0.7	0.3	0.6
disallowed			0.2	0.1	0	0.3	0.6
rmsd							
bonds (Å)			0.008	0.007	0.013	0.013	0.012
angles (deg)			1.045	1.005	1.325	1.371	1.371
PDB code			1XK6	1XK7	1XVT	1XVU	1XVV

7.8 or under conditions similar to those used in crystallization (0.675 M sodium citrate and 50 mM Tris-HCl at pH 7.0) with either 5 mM butyryl- or crotonoyl-CoA in the presence or absence of 5 mM carnitine (Fluka Chemical Co.). Reactions were incubated at 21 °C for a minimum of 24 h. Parallel incubations in the absence of enzyme were performed and used as controls. For TLC, 1 μL of reaction products was spotted on a TLC plate (silica gel), developed in a solvent system consisting of *n*-butanol/water/acetic acid (52:28:20%, v/v) and spots were visualized under UV light. CoA and CoA-thioesters were run in parallel and used to determine R_f values. From the same reaction mixtures, 1 μL of reaction products was diluted 25-fold with HPLC water, 4 μL was injected onto a Zorbax 300SB C18 column, and products were eluted with water/acetonitrile containing 10 mM ammonium formate. CoA and CoA-thioesters were detected using a diode-array detector to record on-line spectra of the elution peaks. Mass spectra were acquired in negative mode and analyzed using Agilent ChemStation software (version A.09.01).

PDB Accession Codes. Coordinates of apo-CaiB, its complex with CoA, and bound to carnitinyl-CoA have been deposited in the RCSB Protein Data Bank (*36*) with PDB codes 1XK6 (apo-CaiB, space group *P*1), 1XK7 (apo-CaiB, space group *C*2), 1XVT (CaiB-CoA, space group $P4_12_12$), 1XVU (CaiB(Asp169Ala)-CoA, space group $P4_12_12$), and 1XVV (CaiB(Asp169Ala)-carnitinyl CoA, space group $P4_12_12$).

RESULTS AND DISCUSSION

Quality of the Refined CaiB Models. Apo-CaiB was crystallized in two forms, space groups *P*1 and *C*2, and the latter model was refined to 1.6 Å resolution with good stereochemistry (Table 1). Each molecule of apo-CaiB includes residues 4−405 (*P*1 crystal form) or residues 1−405 together with the N-terminal residues Ser-His originating from the pGEX-4T1 vector following cleavage of the fusion protein with thrombin (*C*2 crystal form). Two residues with well-defined electron density, Glu23 and Asp76, in both the *P*1 and *C*2 models of apo-CaiB are found in the disallowed region of the Ramachandran plot, as determined using PROCHECK (*37*).

The cosubstrates of CaiB, crotonobetainyl-CoA and *γ*-butyrobetainyl-CoA (*13*), are not available commercially, although similar ligands lacking the betaine moiety, $N(CH_3)_3^+$, namely, butyryl-CoA and crotonoyl-CoA, are available (Figure 1). Cocrystallization of apo-CaiB with either CoA or crotonoyl-CoA yielded crystals that contained only bound CoA. Crystals of CaiB were also obtained in the presence of butyryl-CoA, but they did not diffract to sufficiently high

resolution and were not characterized further. Because CoA but not intact crotonoyl-CoA was observed in electron-density maps for apo-CaiB cocrystallized with crotonoyl-CoA, an active-site mutant CaiB enzyme, Asp169Ala, was prepared, purified, and crystallized with CoA derivatives. As expected from the DNA sequence of the mutant, electron density was visible only up to Cβ at residue 169, confirming the presence of Ala at this position. Crystals of the Asp169Ala mutant cocrystallized with crotonoyl-CoA showed electron density only for the CoA portion. When both crotonoyl-CoA and carnitine were cocrystallized with the Asp169Ala mutant of CaiB, the observed electron density extended beyond the CoA moiety and was interpreted as the structure of carnitinyl-CoA instead. Attempts to obtain a complex with bound carnitine alone, either by soaking or cocrystallization with either apo-CaiB or the Asp169Ala mutant, with or without CoA or its derivatives, were unsuccessful. As in previous studies of *E. coli* YfdW, attempts to form a ternary complex with the cofactor and substrate have been either unsuccessful (*22*) or have yielded a nonproductive complex with the substrate (*23*).

In tetragonal crystals containing either bound CoA or carnitinyl-CoA, some surface regions of the large domain not involved in crystal contacts, including residues 4−16, 46−49, 69−90, 100−120, 185−193, 345−350, and 367−405, showed less well-defined electron density with most side chains modeled as poly-Ala and therefore have somewhat higher *R* factors than obtained with the apo structures. A substantial decrease in the *R* factors upon applying the TLS correction demonstrated an overall anisotropic motion of molecules in this crystal form. These regions are well-ordered in the better diffracting *P*1 and *C*2 crystal forms, with some of them involved in crystal contacts, and no corrections for anisotropic motion of the molecules were necessary. We also find that corresponding regions of the YfdW and formyl-CoA transferase structures are well-ordered through crystal lattice contacts.

Structure of the CaiB Monomer and Dimer. Apo-CaiB in the *P*1 unit cell contains four monomers, arranged in two dimers. The dimer formed from two interlocked monomers adopts an unusual architecture, which is a hallmark of the class III CoA transferase family (Figure 2) (*21*−*23*). Each monomer consists of a large (residues Met1−Tyr201 and Asn363−Asp405) and a small (residues Gly228−Lys321) domain, at either end of an oval-shaped ring (90 × 45 × 30 Å) with a hole in the middle, connected by two linkers, Glu202−Lys227 (Lnk1) and Val322−Asn362 (Lnk2) (Figure 2a). The first 201 residues of the large domain adopt an $\alpha/\beta/\alpha$ structure with a Rossmann fold containing a six-stranded β sheet and two helices on each side of the sheet. The small domain consists of a 4-stranded, antiparallel β sheet, flanked on the solvent side by three helices. A long loop connects helices 2 and 3. The structures of the individual apo-CaiB monomers and dimers are very similar in the two crystal forms. A comparison of the seven individual apo-CaiB monomers in the two crystal forms showed that the root-mean-square deviation (rmsd) for main-chain atoms is within 0.19−0.36 Å, indicating that the structure of apo-CaiB monomers or dimers does not differ significantly between the two packing environments.

CaiB forms dimers, both in solution as we observe by dynamic light scattering and as shown previously by gel filtration (*11*) and in the crystal. In the dimer, the two large domains from each chain interact closely, with the concave sides of the two β sheets facing each other. The long helices lining this face of the sheet form an angle of ~15° and provide the main contacts. The small domains face the large domains from the opposite monomer but make very few direct interactions with them or with each other (Figure 2b). A cleft, which represents the location of the active site, is located between the large and small domains of the two monomers that form the dimer.

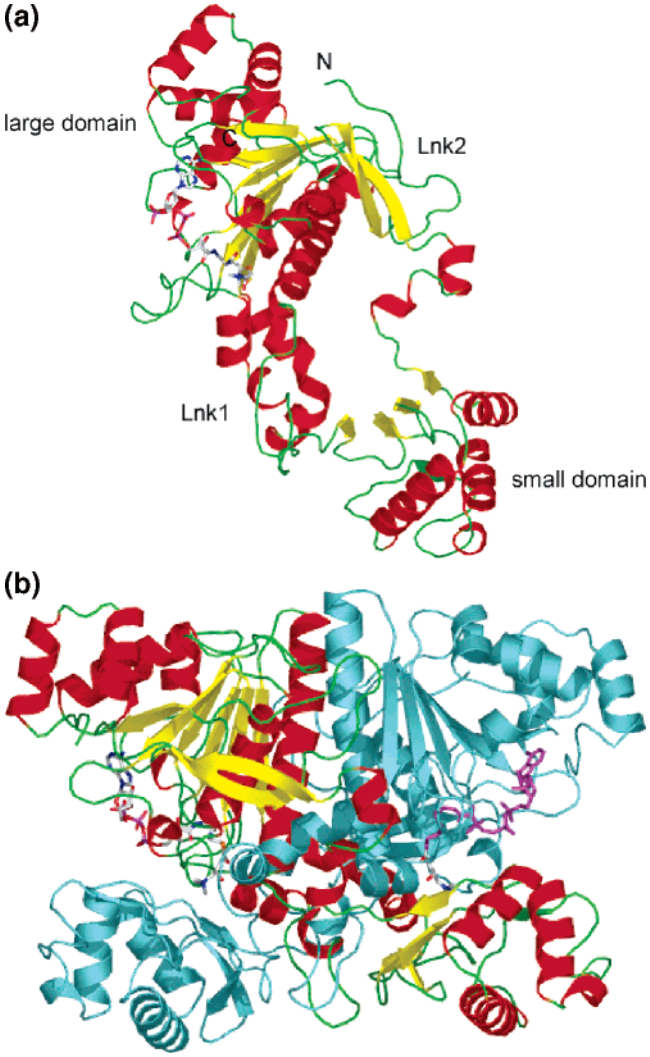

FIGURE 2: Structure of the CaiB monomer and dimer. (a) Ribbon representation of the monomer, showing the larger, N-terminal domain containing the Rossmann fold (top) and the smaller, C-terminal domain (bottom). The carnitinyl-CoA is shown in a stick representation. (b) Structure of the CaiB dimer. One monomer is colored according to the secondary structure, with helices in red and β strands in yellow, while the second monomer is colored cyan. Figures were prepared using PyMOL (www.pymol.org).

Comparison with Other Family III CoA Transferases. The structures of two other enzymes belonging to the class III CoA transferase family are presently known, namely, formyl-CoA transferase from *Oxalobacter formigenes* (PDB code 1P5H, *21*) and a putative formyl-CoA transferase YfdW from *E. coli* (PDB code 1Q6Y, *23*). These two proteins display 57% amino acid sequence identity, and their structures superimpose very well. The only significant difference between them is that the loop in the Lnk1 linker in the *O. formigenes* enzyme is 10 residues longer (Asn232−Leu241)

FIGURE 3: Superposition of monomers of apo-CaiB (PDB 1XK6, —), formyl-CoA transferase (PDB 1Q6Y, ···), and *E. coli* YfdW (PDB 1P5H, - - -). Structures were superposed using Deep View (*41*).

than the corresponding loop in YfdW. Like CaiB, they associate into intertwined dimers. The precise function of YfdW remains unknown, although its fold and sequence suggest it is a member of the class III CoA transferases. Although *E. coli* CaiB and *O. formigenes* formyl-CoA transferase share only 22% overall sequence identity, they have very similar structures, as was originally predicted for family III CoA transferases (*23*). The rmsd between these two apo structures is 1.50 Å for 280 Cα atoms (Figure 3). Similarly, the superposition of CaiB and YfdW gives an rmsd of 1.40 Å for 250 Cα atoms with a sequence identity of 25%. A comparison of CaiB and formyl-CoA transferase shows that the above-mentioned loop in the Lnk1 linker is shorter by 29 residues than in formyl-CoA transferase. In addition, there is a small insertion of ~8 residues in CaiB near residue Gln55. The Rossmann fold domains are very well structurally conserved between formyl-CoA transferase and CaiB, and indeed, the sequence identity in the first 200 residues is ~28%. Interestingly, the residues conserved in ~90 related sequences (Pfam family PF02515) are located within the β strands and on the sides of helices contacting the strands of the β sheet with very few conserved residues involved in dimer-forming contacts. Superposition of the small domains of formyl-CoA transferase (PDB 1P5H) and CaiB, while similar in structure, show more variations than for the larger, Rossmann fold domain. The main difference is in the region (275−285) of CaiB, where the local structures in CaiB and the other two proteins are different. In addition, the segment 250−296 has a slightly different orientation relative to the small β sheet in CaiB and in the other proteins. The linker Lnk2 and the C terminus that forms part of the large domain are quite similar in all three proteins.

The comparison of dimers of CaiB and formyl-CoA transferase shows that the disposition of the small domain relative to the large domain is somewhat different, largely because of the presence of a large insertion in the Lnk1 region of formyl-CoA transferase corresponding to a rotation of ~10° along the pseudo 2-fold axis of the dimer.

Structures of CaiB and the Asp169Ala Mutant Bound to CoA. Efforts to soak CoA into *P*1 crystals of CaiB did not yield an enzyme−cofactor complex. Cocrystallization of CaiB with CoA or crotonoyl-CoA did yield a different crystal form under different conditions compared to apo-CaiB. Unlike apo-CaiB crystals, however, which grew to their final size within a week, cocrystals of CaiB with CoA alone, crotonyl-CoA, or butyryl-CoA took several weeks to grow to their final size. Crystals of wild-type CaiB cocrystallized with CoA alone showed the expected electron density consistent with this ligand (result not shown). Surprisingly, crystals grown in the presence of crotonoyl-CoA also showed electron density for only the CoA moiety (Figure 4a), indicating that CaiB is capable of hydrolysis of crotonoyl-CoA.

CoA binds within a deep pocket formed between the large domain of one monomer and the small domain of the second monomer making contacts almost exclusively with the large Rossmann fold domain. Much of the adenine ring portion of the cofactor appears solvent-exposed, unlike in formyl-CoA transferase where the ring is wedged in a thin cleft (*21*). In CaiB, water-mediated hydrogen bonds (<3.6 Å) are formed between $Ser20^{OG}$ and N7 and N6 atoms of the adenine base. The base is also anchored through a hydrogen bond between Leu71 O and N6. The phosphoribose forms hydrogen bonds with $Arg104^{NE}$ and $Arg104^{NH2}$ as well as $Lys97^{NE}$. The second phosphoryl group also forms a hydrogen bond with $Lys97^{NE}$. The N4 atom of the pantothenic moiety makes a hydrogen bond with Ala139 O. Finally, the terminal S atom is hydrogen-bonded to Asp169, as well as to Ile24 N. A number of van der Waals contacts are also formed between the protein and CoA, including the side chains of Ala25, Tyr140, and Met200 that form the binding site for the cysteamine portion of CoA. The only close

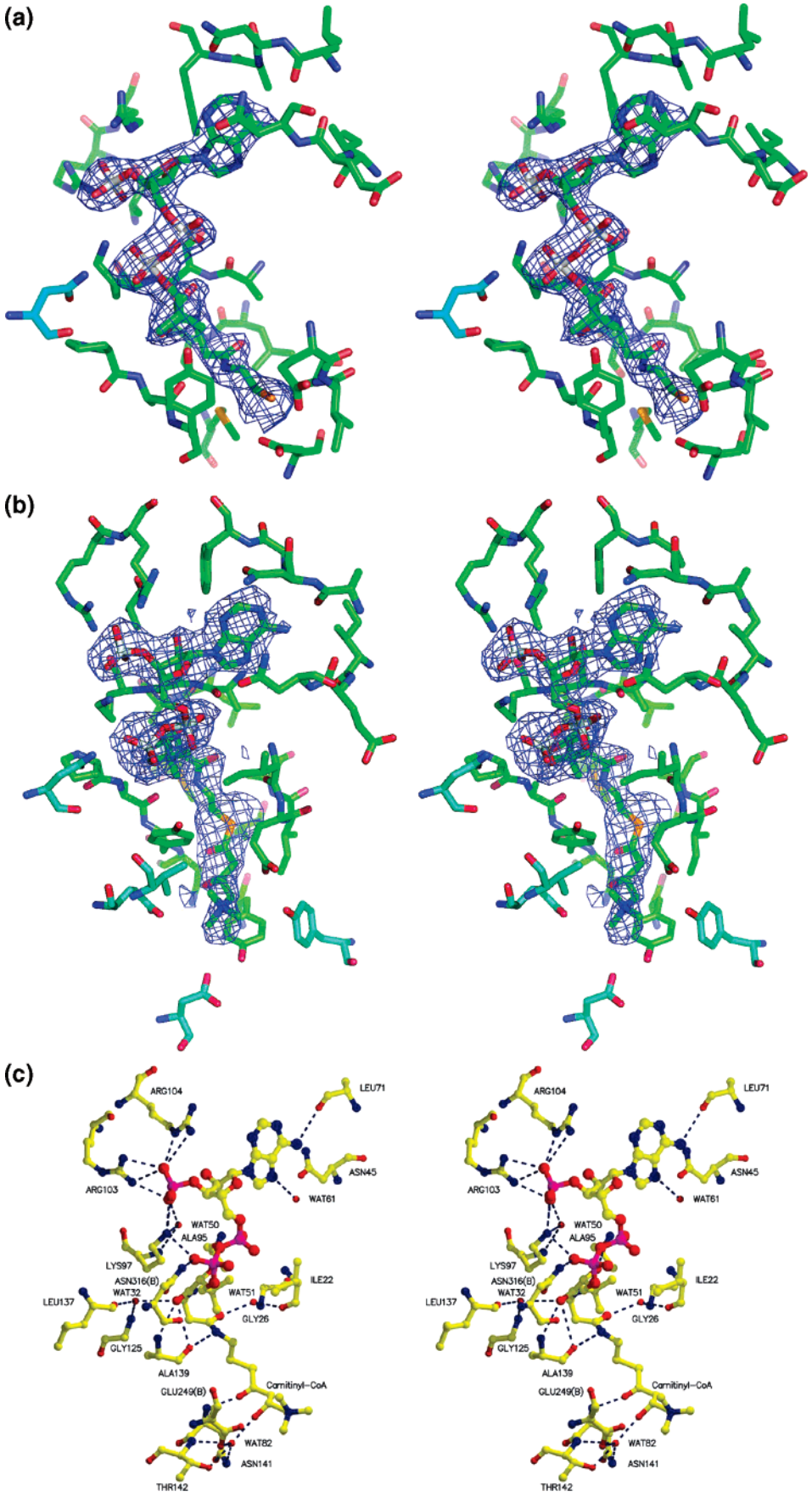

FIGURE 4: Binding of CoA and carnitinyl-CoA to CaiB. (a) $F_o - F_c$ omit map (CoA omitted prior to refinement) for wild-type CaiB cocrystallized with crotonoyl-CoA, with the final model of CoA superposed. This map and the one in b are contoured at a level of 2.5σ. (b) $F_o - F_c$ omit map (carnitinyl-CoA omitted prior to refinement) for the Asp169Ala mutant of CaiB cocrystallized with crotonoyl-CoA and carnitine, showing electron density for carnitinyl-CoA. (c) Interactions between CaiB and carnitinyl-CoA. Hydrogen-bonding interactions are indicated by dashed lines.

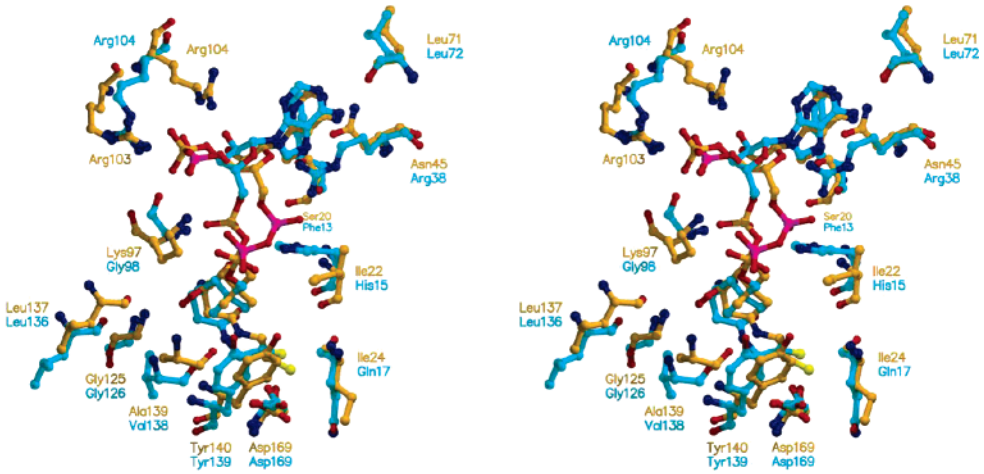

FIGURE 5: Comparison of CoA-binding sites in CaiB and formyl-CoA transferase. Superposition of the CoA-binding regions of CaiB (orange, PDB 1XVT) and formyl-CoA transferase (cyan, PDB 1T4C).

contact with the small domain is between Asn316^{ND2} from the second monomer and the O4 and O5 atoms of the phosphoryl group. These hydrogen-bonding interactions are summarized in Figure 4c. Superposition of the CoA-binding sites of CaiB and formyl-CoA transferase (Figure 5) reveals that the location of CoA binding is very similar in each case, although the pantethenoyl moiety of CoA adopts a somewhat more extended conformation in the CaiB-CoA complex than in formyl-CoA transferase. However, some of the specific protein-CoA contacts are different comparing CaiB and the other structures, in part reflecting the low overall sequence identity between these two proteins.

The sequence conservation of Asp169 and its close position relative to the terminal S atom of CoA in the available crystal structures of class III CoA-transferases suggested it to be a key catalytic residue (*21*−*23*). Superposition of CaiB with the formyl-CoA transferase reveals a very similar position of the Asp169 side chain in the two structures (Figure 5). In an effort to obtain crystals with the intact cosubstrate, we constructed the Asp169Ala mutant of CaiB, in which the predicted key catalytic residue Asp169 (*21*, *22*, *24*) was mutated to alanine. This protein was produced, purified, and cocrystallized with CoA derivatives. With crotonoyl-CoA, electron density is observed only for the CoA region of the cofactor, ending at the sulfur atom (result not shown) as for the wild-type enzyme, suggesting that this mutant possesses residual hydrolytic activity. This corroborates a recent report that the same Asp169Ala mutation of formyl-CoA transferase from *O. formigenes* does not completely inactivate the enzyme but reduces the catalytic rate by ~1300-fold (*24*).

Structure of CaiB Asp169Ala with Carnitinyl-CoA. When both carnitine and crotonoyl-CoA were cocrystallized with the CaiB Asp169Ala mutant enzyme, the electron density observed in the binding site was consistent with formation of the product, carnitinyl-CoA (Figure 4b). Formation of carnitinyl-CoA could also be observed when the Asp169Ala mutant enzyme was cocrystallized with butyryl-CoA and carnitine, although the electron density for the carnitinyl moiety was weaker in this case. In addition to the interactions previously described for bound CoA, the positive charge of the quaternary amine moiety of carnitinyl-CoA is proximal to the side chains of Glu23^{A} (superscript refers to the chain) and Glu249^{B} (small domain), thereby serving to neutralize this charge in an otherwise hydrophobic environment. The carbonyl O atom of carnitine is anchored through a hydrogen bond with the amide NH of Asn141^{A}. The three methyl groups of the betaine moiety are adjacent to a cluster of hydrophobic residues, including Tyr140^{A}, Tyr166^{A}, Cys236^{B}, Val251^{B}, and Leu280^{B}. All of the residues that make interactions with the carnitinyl moiety, with the exception of Tyr140^{A}, are found only in sequences closely related to CaiB.

Comparison of CoA-Bound and -Free Structures. The active-site cleft of CaiB is observed to close partially upon binding of CoA or its derivatives. A comparison of CaiB in apo- and CoA-bound forms reveals that the small domain rotates approximately 15° as a result of CoA binding (Figure 6). Superposition of the two models gives an overall rmsd of 1.1 Å for all Cα atoms. The domain movements observed upon binding of CoA seems to be unique to CaiB, because this is not observed in other class III CoA transferase structures. Rather, in these structures, only movement of the glycine-rich loop (Gly258−261 of formyl-CoA transferase or Gly246−249 of YfdW), a part of the C-terminal domain, occurs upon CoA binding (*21*−*24*). In CaiB, there is no glycine-rich loop, but instead, a loop consisting of residues Asp230−Cys236 is found at an equivalent position and is more closely packed against the C-terminal domain, resulting in a more open active-site cleft in CaiB than in the other two CoA-transferases. Unlike in YfdW and formyl-CoA transferase, this loop retains essentially the same conformation in apo- and CoA-bound forms of CaiB.

Mechanism of Catalysis. The observation of only CoA in the structure of CaiB cocrystallized with crotonoyl-CoA suggested that the enzyme has the ability to hydrolyze this CoA derivative. Indeed, both TLC and LC−ESI−MS analysis of either crotonoyl-CoA (peak at MW = 835 Da) or butyryl-CoA (peak at MW = 837 Da) after 3 days of incubation showed the formation of free CoA (peak at MW = 767 Da) in the presence of wild-type CaiB. Additional LC−MS experiments showed that butyryl-CoA is a relatively stable compound, not releasing detectable CoA up to incubation times of as much as 10 days. A similar observation of only bound CoA in the structure of the CaiB Asp169Ala mutant cocrystallized with crotonoyl-CoA is consistent with the ability of this mutant enzyme to release free CoA from crotonoyl-CoA as also confirmed by TLC

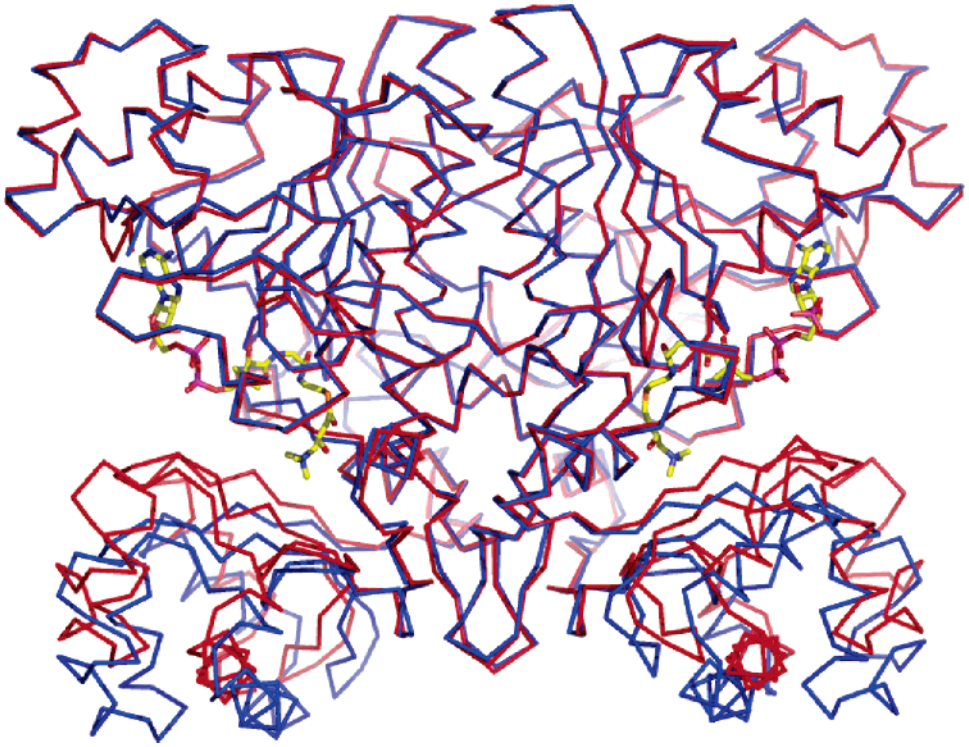

FIGURE 6: Structural superposition of dimers of apo-CaiB (blue) and CaiB-carnitinyl-CoA (red) showing the domain movement observed upon CoA binding. Carnitinyl-CoA is shown in a stick representation.

and LC−ESI−MS. Together, our biochemical and structural data show that wild-type and mutant CaiB are able to catalyze release of CoA from crotonoyl-CoA. This hydrolysis reaction could occur via activation of a water molecule using Asp169 (wild-type CaiB) or Glu23 (Asp169Ala mutant) as a general base, as shown previously with *Acidaminococcus fermentans* glutaconate CoA-transferase (*38*).

Surprisingly, in crystals of this mutant cocrystallized with crotonoyl-CoA and carnitine, we observed electron density that extended beyond the CoA and that was interpreted as carnitinyl-CoA. In the study of formyl-CoA transferase (*24*), the suggestion was put forth that the enzyme−substrate−cofactor ternary complex could, even in the absence of Asp169, undergo catalysis leading to formation of the product, although at a much lower rate (ca. 1300-fold) compared with the wild-type enzyme. Our observations suggest that, in the absence of the nucleophile provided by the protein, catalysis could proceed through the formation of a ternary complex, which would allow for a direct attack of carnitine on the CoA substrate, as previously proposed for other family III CoA transferases (*15*, *24*). We cannot, however, rule out the possibility that carnitine attacks crotonoyl-CoA in solution, yielding carnitinyl-CoA, which in turn binds to the enzyme, or that another residue in the active-site region, such as Glu23, substitutes catalytically for Asp169 in the mutant enzyme. In the CaiB-carnitinyl-CoA complex, the side-chain O atom of Glu23 is 4.5 Å from the carbonyl carbon of the anhydride. A small rotation of this side chain by about 25° would place it within a suitable distance for nucleophilic attack.

Two other residues, Tyr59 and Gln17 of formyl-CoA transferase, have been suggested to participate in stabilizing the tetrahedral intermediates through hydrogen-bonding interactions (*24*). We find that neither of these residues is structurally conserved in CaiB. Tyr58 of CaiB is approximately 8.0 Å removed from Tyr59 of formyl-CoA transferase, while with Gln17, the residue Ile24 is found at this position in CaiB. These observations, in addition to the absence of a flexible loop in CaiB equivalent to the glycine-rich loop of formyl-CoA transferase, which has been implicated in playing a role in catalysis (*24*), highlight additional differences between these two enzymes.

The CaiB-CoA structure is in agreement with the previously proposed reaction mechanism employing a series of aspartyl anhydride intermediates (*24*). This would be expected to be the preferred route to product formation in CaiB, as with other members of the class III CoA transferases, accelerating catalysis considerably compared with direct attack of one substrate on the other. Whether the chemical mechanism employs aspartyl anhydride formation or direct attack of one substrate on the other, formation of an enzyme−substrate ternary complex is expected. The kinetic mechanism of formyl-CoA transferase has been shown to be ordered Bi−Bi, involving an enzyme−cofactor−substrate ternary complex in which formyl-CoA binds prior to oxalate at the active site (*24*). With both succinyl-CoA:(*R*)-benzysuccinate CoA-transferase (*17*) and cinnamoyl-CoA:phenyllactate CoA transferase (*18*), kinetic analysis also suggests a ternary enzyme−substrate complex, although with the absence of a covalent enzyme-bound intermediate. This kinetic mechanism is distinct from that of class I CoA transferases, which utilize a ping-pong mechanism (*39*). While no data on the kinetic mechanism of CaiB are available, one similar to that of other class III CoA-transferases, in which a ternary complex is formed, is likely (*17*, *18*, *24*).

Oxalate is a small substrate and could presumably be accommodated within the active site of formyl-CoA transferase in the ternary complex with only small, local structural changes. We do not observe an obvious betaine-binding site

in the CaiB-carnitinyl-CoA complex that could accommodate the second substrate of the reaction without causing steric clashes with the enzyme. The betainyl derivatives used by CaiB, being larger than oxalate, would likely require greater structural changes to form the enzyme−substrate ternary complex. Inspection of the CaiB-carnitinyl-CoA complex suggests that a repositioning of the small and large domains of opposing monomers, where the active-site cleft is formed, would be the most obvious way to accommodate the ternary complex. It is noteworthy in this regard that CaiB but not formyl-CoA transferase or YfdW exhibits closure of the small and large domains upon CoA or carnitinyl-CoA binding.

ACKNOWLEDGMENT

We thank Robert Larocque for cloning the *caiB* gene, as well as Véronique Sauvé for protein crystallization. We also thank Robert Menard for useful discussions on the catalytic mechanism. Data for this study were measured at beamlines X8C and X25 of the National Synchrotron Light Source. Financial support comes principally from the Office of Biological and Environmental Research and of Basic Energy Sciences of the U.S. Department of Energy and the National Center for Research Resources of the National Institutes of Health. We thank Leonid Flaks (beamline X8C) and Michael Becker (beamline X25) for assistance in data collection.

NOTE ADDED IN PROOF

Simultaneous with the submission of this manuscript, the crystal structure of *E. coli* CaiB and its complex with CoA were reported (*40*). There is good agreement between the two sets of structures, with a rmsd of 0.72 Å between apo-CaiB dimers for all main-chain atoms (PDB 1XK6 and 1XA3), and 0.73 Å between the CaiB-CoA complexes (PDB 1XVT and 1XA4). The CoA-induced domain movement has been identified independently in the two studies. The locations of the N atoms of the tertiary-amine group of the bis-tris molecule (*40*) and carnitine (this paper) agree very well, confirming the location of the carnitine-binding site.

REFERENCES

1. Bieber, L. L. (1988) Carnitine, *Annu. Rev. Biochem. 57*, 261−283.
2. Verheul, A., Wouters, J. A., Rombouts, F. M., and Abee, T. (1998) A possible role of ProP, ProU, and CaiT in osmoprotection of *Escherichia coli* by carntine, *J. Appl. Microbiol. 8*, 1036−1046.
3. Emaus, R. K., and Bieber, L. L. (1983) A biosynthetic role for carnitine in the yeast *Torulopsis biovina*, *J. Biol. Chem. 258*, 13160−13165.
4. Obon, J. M., Maiquez, J. R., Canovas, M., Kleber, H.-P., and Iborra, J. L. (1999) High-density *Escherichia coli* cultures for continuous L-(−)-carnitine production, *Appl. Microbiol. Biotechnol. 51*, 760−764.
5. Jung, H., and Kleber, H.-P. (1993) Synthesis of L-carnitine by microorganisms and isolated enzymes, *Adv. Biochem. Eng. 50*, 21−44.
6. Kleber, H.-P. (1997) Bacterial carnitine metabolism, *FEMS Microbiol. Lett. 147*, 1−9.
7. Seim, H., Loster, H., Claus, R., Kleber, H.-P., and Strack, E. (1982) Splitting of the C−N bond in carnitine by an enzyme (trimethylamine-forming) from membranes of *Acinetobacter calcoaceticus*, *FEMS Microbiol. Lett. 15*, 165−167.
8. Eichler, K., Bourgis, F., Buchet, A., Kleber, H.-P., and Mandrand-Berthelot, M.-A. (1994) Molecular characterization of the *cai* operon necessary for carnitine metabolism in *Escherichia coli*, *Mol. Microbiol. 13*, 775−786.
9. Buchet, A., Nasser, W., Eichler, K., and Mandrand-Berthelot, M.-A. (1999) Positive co-regulation of the *Escherichia coli* carnitine pathway *cai* and *fix* operons by CRP and CaiF activator, *Mol. Microbiol. 34*, 562−575.
10. Jung, H., Jung, K., and Kleber, H.-P. (1989) Purification and properties of carnitine dehydratase from *Escherichia coli*−A new enzyme of carnitine metabolization, *Biochim. Biophys. Acta 1003*, 270−276.
11. Preusser, A., Wagner, U., Elssner, T., and Kleber, H.-P. (1999) Crotonobetaine reductase from *Escherichia coli* consists of two proteins, *Biochim. Biophys. Acta 1431*, 166−178.
12. Elssner, T., Engemann, C., Baumgart, K., and Kleber, H.-P. (2001) Involvement of coenzyme A esters and two new enzymes, an enoyl-CoA hydratase and a CoA-transferase, in the hydration of crotonobetaine to L-carnitine by *Escherichia coli*, *Biochemistry 40*, 11140−11148.
13. Elssner, T., Hennig, L., Frauendorf, H., Haferburg, D., and Kleber, H.-P. (2000) Isolation, identification, and synthesis of γ-butyrobetainyl-CoA and crotonobetainyl-CoA, compounds involved in carnitine metabolism of *E. coli*, *Biochemistry 39*, 10761−10769.
14. Engemann, C., Elssner, T., and Kleber, H.-P. (2001) Biotransformation of crotonobetaine to L-(−)-carnitine in *Proteus* sp, *Arch. Microbiol. 175*, 353−359.
15. Heider, J. (2001) A new family of CoA-transferases. *FEBS Lett. 509*, 345−349.
16. Baetz, A. L., and Allison, M. J. (1990) Purification and characterization of formyl-coenzyme A transferase from *Oxalobacter formigenes*, *J. Bacteriol. 172*, 3537−3540.
17. Leutwein, C., and Heider, J. (2001) Succinyl-CoA:(*R*)-benzylsuccinate CoA-transferase: An enzyme of the anaerobic toluene catabolic pathway in denitrifying bacteria, *J. Bacteriol. 183*, 4288−4295.
18. Dickert, S., Pierik, A., Linder, D., and Buckel, W. (2000) The involvement of coenzyme A esters in the dehydration of (*R*)-phenyllactate to (*E*)-cinnamate by *Clostrium sporogenes*, *Eur. J. Biochem. 267*, 3874−3884.
19. Bateman, A., Coin, L., Durbin, R., Finn, R. D., Hollich, V., Griffiths-Jones, S., Khanna, A., Marshall, M., Moxon, S., Sonnhammer, E. L. L., Studholme, D. J., Yeates, C., and Eddy, S. R. (2004) The Pfam protein families database, *Nucleic Acids Res. 32*, D138−D141.
20. White, W. B., Franklund, C. V., Coleman, J. P., and Hylemon, P. B. (1988) Evidence for a multigene family involved in bile acid 7-dehydroxylation in *Eubacterium* sp. strain VP1 12708, *J. Bacteriol. 170*, 4555−4561.
21. Ricagno, S., Jonsson, S., Richards, N., and Lindqvist, Y. (2003) Formyl-CoA transferase encloses the CoA binding site at the interface of an interlocked dimer, *EMBO J. 22*, 3210−3219.
22. Gogos, A., Gorman, J., and Shapiro, L. (2004) Structure of *Escherichia coli* YfdW, a type III CoA transferase, *Acta Crystallogr., Sect. D 60*, 507−511.
23. Gruez, A., Roig-Zamboni, V., Valencia, C., Campanacci, V., and Cambillau, C. (2003) The crystal structure of the *Escherichia coli* YfdW gene product reveals a new fold of two interlaced rings identifying a wide family of CoA transferases, *J. Biol. Chem. 278*, 34582−34586.
24. Jonsson, S., Ricagno, S., Lindqvist, Y., and Richards, N. G. J. (2004) Kinetic and mechanistic characterization of the formyl-CoA transferase from *Oxalobacter formigenes*, *J. Biol. Chem. 279*, 36003−36012.
25. Eichler, K., Wolf-Hagen, S., Kleber, H.-P., and Mandrand-Berthelot, M.-A. (1994) Cloning, nucleotide sequence, and expression of the *Escherichia coli* gene encoding carnitine dehydratase, *J. Bacteriol. 176*, 2970−2975.
26. Hendrickson W. A., Horton J. R., and LeMaster, D. M. (1990) Selenomethionyl proteins produced for analysis by multiwavelength anomalous diffraction (MAD): A vehicle for direct determination of three-dimensional structure, *EMBO J. 9*, 1665−1672.
27. Otwinowski, Z., and Minor, W. (1997) Processing of X-ray diffraction data collected in oscillation mode, *Methods Enzymol. 276*, 307−326.
28. Terwilliger, T. C., and Berendzen, J. (1999) Automated MAD and MIR structure solution, *Acta Crystallogr., Sect. D 55*, 849−861.
29. Terwilliger, T. C. (2000) Maximum-likelihood density modification, *Acta Crystallogr., Sect. D 56*, 965−972.

30. Murshudov G. N., Vagin A. A., Lebedev A., Wilson K. S., and Dodson, E. J. (1999) Efficient anisotropic refinement of macromolecular structures using FFT, *Acta Crystallogr., Sect. D 55*, 247−255.
31. Jones, T. A., Zou, J.-Y., Cowan, S., and Kjeldgaard M. (1991) Improved methods for building protein models in electron density maps and the location of errors in these models, *Acta Crystallogr., Sect. A 47*, 100−119.
32. Vagin A. A., and Isupov, M. N. (2001) Spherically averaged phased translation function and its application to the search for molecules and fragments in electron-density maps, *Acta Crystallogr., Sect. D 57*, 1451−1456.
33. Winn, M. D., Ashton, A. W., Briggs, P. J., Ballard, C. C., and Patel, P. (2002) Ongoing developments in CCP4 for high-throughput structure determination, *Acta Crystallogr., Sect. D 58*, 1929−1936.
34. Winn, M. D., Murshudov, G. N., and Papiz, M. Z. (2003) Macromolecular TLS refinement in REFMAC at moderate resolution, *Methods Enzymol. 374*, 300−321.
35. Winn, M. D., Isupov, M. N., and Murshudov, G. N. (2001) Use of TLS parameters to model anisotropic displacements in macromolecular refinement, *Acta Crystallog., Sect. D 57*, 122−133.
36. Berman, H. M., Westbrook, J., Feng, Z., Gilliland, G., Bhat, T. N., Weissig, H., Shindyalov, I. N., and Bourne, P. E. (2000) The Protein Data Bank, *Nucleic Acids Res. 28*, 235−242.
37. Laskowski, R. A., McArthur, M. W., Moss, D. S., and Thornton, J. M. (1993) PROCHECK: A program to check the stereochemical quality of protein structures, *J. Appl. Crystallog. 26*, 282−291.
38. Selmer, T., and Buckel, W. (1999) Oxygen exchange between acetate and the catalytic glutamate residue in glutaconate CoA-transferase from *Aciaminococcus fermentans*, *J. Biol. Chem*. 274, 20772−20778.
39. White, H., and Jencks, W. P. (1976) Mechanism and specificity of succinyl-CoA:3-ketoacid coenzyme A transferase, *J. Biol. Chem. 251*, 1688−1699.
40. Stenmaek, P., Gurmu, D., and Nordlund, P. (2004) Crystal structure of CaiB, a type-III CoA transferase in carnitine metabolism, *Biochemistry 43*, 13996−14003.
41. Guex, N., and Peitsch, M. C. (1997) SWISS-MODEL and the Swiss-Pdb viewer: An environment for comparative protein modeling, *Electrophoresis 18*, 2714−2723.

BI047656F